MADRID
inter.noise 2019
June 16 - 19
NOISE CONTROL FOR A BETTER ENVIRONMENT

3D analysis of sonic crystal structures with absorbing scatterers

Godinho, Luís[1]
ISISE, Department of Civil Engineering, University of Coimbra
R. Luis Reis dos Santos 290, 3030-790 Coimbra, Portugal

Redondo, Javier[2]
Instituto de Investigación para la Gestión Integrada de
Zonas Costeras, Gandia, Universitat Politècnica de València, Spain

Amado-Mendes, Paulo[3]
ISISE, Department of Civil Engineering, University of Coimbra
R. Luis Reis dos Santos 290, 3030-790 Coimbra, Portugal

ABSTRACT

Computer simulation of sonic crystals using realistic 3D models is a demanding task. Indeed, most of the published works correspond to 2D problems, and only a few deal with the 3D character of such structures. The present paper presents an efficient method based on the Method of Fundamental Solutions (MFS) to deal with sonic crystals made of 3D scatterers, infinitely repeated with constant spacing along one direction. The method makes use of a special form of the acoustic fundamental solutions which can be highly efficient in such analysis, while allowing just the cell that is repeated to be effectively modelled. Verification of the model is provided by comparing its results with those from a FDTD algorithm. Absorbing surfaces are considered by means of imposing impedance surface conditions. A simulation example is presented to evidence the formation of acoustic band-gaps at specific frequency bands associated with the Bragg effect, and to illustrate the effect of scatterer absorption.

Keywords: 3D, MFS, sonic crystal, infinite periodic structure
I-INCE Classification of Subject Number: 76

1. INTRODUCTION

The numerical analysis of sonic crystals is still a challenge in the technical and scientific community. Since the 1990's some proposals emerged, such as those proposed by Kafesaki and Economou [1], using the Multiple Scattering Theory (MST) to analyse a periodic array of elastic spheres embedded in a fluid medium. Cao et al. [2] and Yan and Wang [3] used plane-wave expansion and wavelet-based methods for the analysis of sonic crystals. More general numerical methods such as the Finite Difference Time

[1] lgodinho@dec.uc.pt
[2] fredondo@fis.upv.es
[3] pamendes@dec.uc.pt

Domain (FDTD) Method [4] or the Boundary Element Method (BEM) [5] were also applied to such analyses, particularly in the calculation of the band structure of different sonic crystal configurations. The BEM was also used to study the effect of complementing a traditional noise barrier with a sonic crystal (Koussa et al. [6]). Karimi et al. [7] implemented a so-called Periodic BEM to analyse large arrays of periodically distributed acoustic scatterers. Concerning the Finite Element Method (FEM), it has been applied in the definition of an engineering approach for sonic crystal barrier design, using overlapping two-dimensional FEM models [8]. This approach, however, does not fully incorporate the 3D character of the generated wavefields in 3D sonic crystals.

Meshless methods have recently been applied in the context of sonic crystals. Two examples are the works of Zheng et al. [9], using Radial Basis Functions (RBF) for the analysis of the band structure of in-plane and anti-plane elastic waves in 2D sonic crystals, and of Yan et al. [10], also using RBF-based techniques.

The meshless Method of Fundamental Solutions (MFS) [11,12] is particularly interesting for acoustic analysis. Its concept MFS is quite simple, proposing that the acoustic wavefield in the presence of scatterers can be reproduced by means of the superposition of the effects of multiple sources, each with an a-priori unknown amplitude.

The present paper proposes an approach for the 3D analysis of sonic crystals making use of a highly efficient MFS implementation to deal with sonic crystals made of 3D scatterers, which are infinitely repeated with constant spacing along one direction. For that purpose, a special form of the acoustic fundamental solution for acoustic problems is used, developed by the authors [13], which can be highly efficient in such analysis. Indeed, by using such periodic fundamental solution only a very small portion of the structure needs to be modelled, corresponding to the unitary cell that is infinitely repeated along one direction. Additionally, in the present work the authors consider the incorporation of surface sound absorption by imposing adequate impedance boundary conditions. Some examples of the influence of this effect are also presented.

2. MFS FORMULATION

The propagation of sound within a three-dimensional space can be mathematically given in the frequency domain by the Helmholtz partial differential equation,

$$\nabla^2 p(\mathbf{x}) + k^2 p(\mathbf{x}) = -\sum_{k=1}^{NS} Q_k \delta(\mathbf{x}_k^f, \mathbf{x}), \tag{1}$$

where $\nabla^2 = \frac{\partial^2}{\partial x^2} + \frac{\partial^2}{\partial y^2} + \frac{\partial^2}{\partial z^2}$; p is the acoustic pressure; $k = \omega/c$; $\omega = 2\pi f$; f is the frequency; c is the sound propagation velocity within the acoustic medium; NS is the number of sources in the domain; Q_k is the magnitude of the existing sources $\mathbf{x}_k^f$ located at (x_k^f, y_k^f, z_k^f); $\mathbf{x}$ is a field point located at (x, y, z); and $\delta(\mathbf{x}_k^f, \mathbf{x})$ is the Dirac delta generalized function.

The boundary conditions for the problem (for $\mathbf{x}$ in the boundary) are given by:

$$v_n(\mathbf{x}) = \frac{\mathrm{i}}{\omega\rho} \frac{\partial p}{\partial \mathrm{n}}(\mathbf{x}) = \overline{v}_n\ (\mathbf{x}) \qquad \text{in interfaces } S_v, \tag{2a}$$

$$p(\mathbf{x}) = \overline{Z}(\mathbf{x}) v_n(\mathbf{x}) \qquad \text{in interfaces } S_Z, \tag{2b}$$

where $\bar{v}_n$ $(\mathbf{x})$ is the normal particle velocity and $\bar{Z}(\mathbf{x})$ is the surface impedance of a possible absorbing material, which are assumed to be known quantities. Eq. (2a) stands for Neumann condition and Eq. (2b) stands for Robin or impedance boundary condition.

Considering that a source point is placed within this propagation domain, at $\mathbf{x}_0$ (x_0, y_0, z_0) , it is possible to establish the fundamental solution for the incident sound pressure at a point $\mathbf{x}$, which can be written as

$$G(\mathbf{x}_0, \mathbf{x}) = \frac{\mathrm{e}^{-\mathrm{i}kr}}{4\pi r}, \text{ with } \quad r = \sqrt{(x-x_0)^2 + (y-y_0)^2 + (z-z_0)^2} \ . \tag{3}$$

In the context of noise barrier analysis, it is usually necessary to consider the effect of the ground plane, which generates an additional reflection that interferes with the expected acoustic results. The presence of a perfectly reflecting plane surface, simulating a rigid ground, can be taken into account by using the well-known image-source method. In this technique, the effect of a source point in the presence of a given plane surface can be simulated by considering an additional virtual source, positioned in a symmetrical position with respect to the reflecting plane. Thus, if such plane is defined by $z = 0$, the corresponding Green's function can be written as

$$G_h(\mathbf{x}_0, \mathbf{x}) = \frac{\mathrm{e}^{-\mathrm{i}kr}}{4\pi r} + \frac{\mathrm{e}^{-\mathrm{i}kr_1}}{4\pi r_1}, \text{ with } r_1 = \sqrt{(x-x_0)^2 + (y-y_0)^2 + (z+z_0)^2}. \tag{4}$$

The Method of Fundamental Solutions is here used to compute the frequency domain response in a three dimensional halfspace surrounding a set of acoustic scatterers. This solution is computed as a linear combination of fundamental solutions for a set of NVS virtual sources, with amplitude A_l (with $l = 1, ..., NVS$). These sources are placed outside the domain of interest (inside the scatterers), to avoid singularities. Thus, the pressure field around the scattering objects can be computed as:

$$p(\mathbf{x}) = \sum_{l=1}^{NVS} A_l G_h\left(\mathbf{x}_l^v, \mathbf{x}\right) + P_{inc}(\mathbf{x}), \tag{5}$$

where the coefficients A_l are unknown amplitudes which are computed by imposing the appropriate boundary conditions at a set of NCP points (collocation points) placed along the surfaces $S = S_v \cup S_Z$ and $G_h\left(\mathbf{x}_l^v, \mathbf{x}\right)$ is the fundamental solution at point $\mathbf{x}$ for a virtual source placed at $\mathbf{x}_l^v$. $P_{inc}(\mathbf{x})$ represents a generic incident wavefield, generated by any source within the acoustic domain. In the MFS model here developed, the Green's function presented in Eq. (4) is used. In this work, an equal number of collocation points and virtual sources is assumed, which allows obtaining a $NVS \times NVS$ system. This system is built by prescribing at each collocation point $\mathbf{x}_m$, placed in the boundaries of the scatterers, the conditions defined in Eq. (2). By applying this procedure one obtains:

$$\sum_{l=1}^{NVS} A_l \frac{\partial G_h\left(\mathbf{x}_l^v, \mathbf{x}_m\right)}{\partial n} = -\frac{\partial P_{inc}(\mathbf{x}_m)}{\partial n}, \tag{6}$$

$$\begin{aligned} &\sum_{l=1}^{NVS} A_l G_h\left(\mathbf{x}_l^v, \mathbf{x}_m\right) + P_{inc}(\mathbf{x}_m) = \\ &\qquad = \frac{\mathrm{i}\overline{Z}(\mathbf{x}_m)}{\rho\omega}\left(\sum_{l=1}^{NVS} \mathrm{A}_l \frac{\partial G_h(\mathbf{x}_l^v, \mathbf{x}_m)}{\partial n} + \frac{\partial P_{inc}(\mathbf{x}_m)}{\partial n}\right). \end{aligned} \tag{7}$$

Eq. (6) is applied for the case of rigid surfaces, while Eq. (7) is employed if it is required to assign absorption to the surfaces of the model. For both cases, a resulting $NVS \times NVS$ system is obtained, which after being solved makes it possible to obtain the acoustic pressure at any point of the domain by applying Eq. (5).

If, instead of the conventional problem described above, a periodic system is considered a periodic fundamental solution for a halfspace can be written as

$$G_{h,per}\left(\mathbf{x}_l^v, \mathbf{x}\right) = \sum_{i=-\infty}^{+\infty} G_h\left(\mathbf{x}_{l,i}^v, \mathbf{x}\right) = -\frac{\mathrm{i}}{4a}\left(\sum_{n=-\infty}^{+\infty}\left(\mathrm{H}_0^{(2)}(k\,'r\,') + \mathrm{H}_0^{(2)}(k\,'r\,'')\right)\mathrm{e}^{-\mathrm{i}\times\frac{2\pi}{a}\times n\times(y-y_0)}\right), \tag{8}$$

where $r'' = \sqrt{(x-x_0)^2 + (z+z_0)^2}$. This summation is known to have good convergence properties, and its derivation can be found in Godinho et al. [13].

3. VERIFICATION OF THE METHOD

For the purpose of verifying the proposed method, a first set of results is presented concerning the insertion loss provided by a sonic crystal structure defined considering a height of 2.0 m and a lattice constant (periodicity) of 0.1715 m; this value is defined so that the theoretical band-gap, generated by the Bragg effect, occurs at f = 343/2/a = 1000 Hz. The incident field corresponds to a plane wave, and the efefct of the the sonic crystal is analyzed by means of its insertion loss, computed as the difference between the average sound pressure levels calculated without and with the structure:

$$IL = L_{without} - L_{with}\ [dB] \tag{9}$$

In the presented IL calculations, the grid of receivers is positioned 0.5 m behind the scatterers. A scheme of the tested configuration is presented in Figure 1.

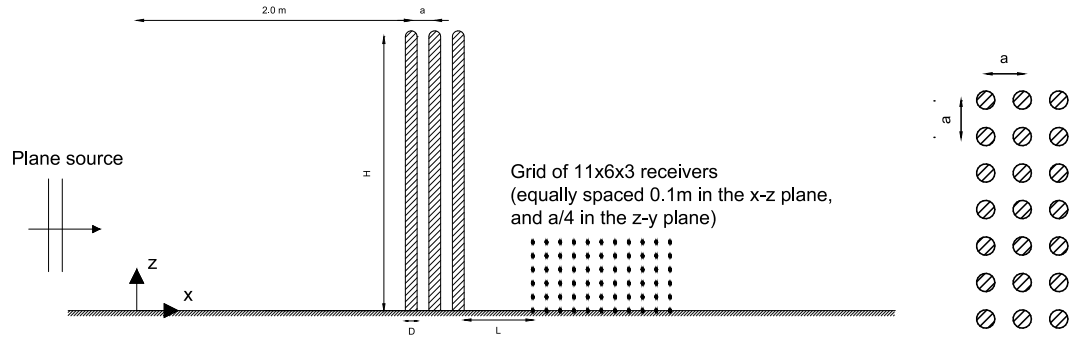

Figure 1 – Side and top views of the sonic crystal.

Figure 2 presents the insertion loss curves calculated in 1/3 octave bands between 100 Hz and 3150 Hz, considering 3 rows of scatterers; for each frequency band, five discrete frequencies are considered. Observing the plot, a first band-gap emerges around 1000 Hz for all configurations, with an IL around 10 dB, occurring at the frequency theoretically estimated considering the Bragg effect. To allow an independent verification of the MFS formulation, the IL was also calculated using a Finite-Difference-Time-Domain (FDTD) algorithm. Further details of the algorithm used can be found at [14]. In that calculation, a spatial step of 0.5 cm was used, equivalent to at least 12 points per wavelength, together with a staggered grid with about 14×10^6 points. Observing the results computed by the two methods, it becomes clear that the same type of behaviour can be identified, with IL peaks occurring at specific frequencies of 1000 Hz and 2500 Hz. The amplitudes of the IL predicted at these frequencies by the MFS and by FDTD are very similar.

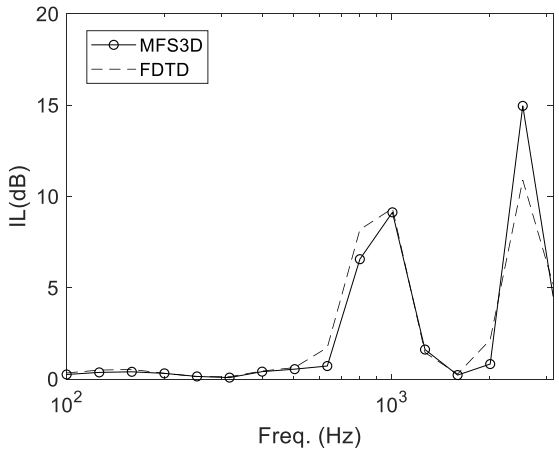

Figure 2 – Insertion loss in 1/3 octave bands computed with FDTD and MFS for sonic crystals 2 m high and 3 rows.

4. NUMERICAL EXAMPLES

In this final section some application examples are presented regarding the performance of sonic crystal sound barriers in what concerns Insertion Loss. For that purpose, the same general scheme already presented in Figure 1 will be adopted.

Figure 3 presents colormap plots representing the sound pressure level registered for a barrier 2.0 m tall, for the incidence of planewaves with 500 Hz and 1000 Hz. One should note that, following the results presented in Figure 2, the lower frequency corresponds to a frequency region where the barrier is of very low efficiency, while the upper frequency corresponds to the first IL peak registered in that figure. Indeed, the colormaps clearly confirm this behaviour, with almost no attenuation being registered at 500 Hz, and with a strong sound reduction being visible at 1000 Hz.

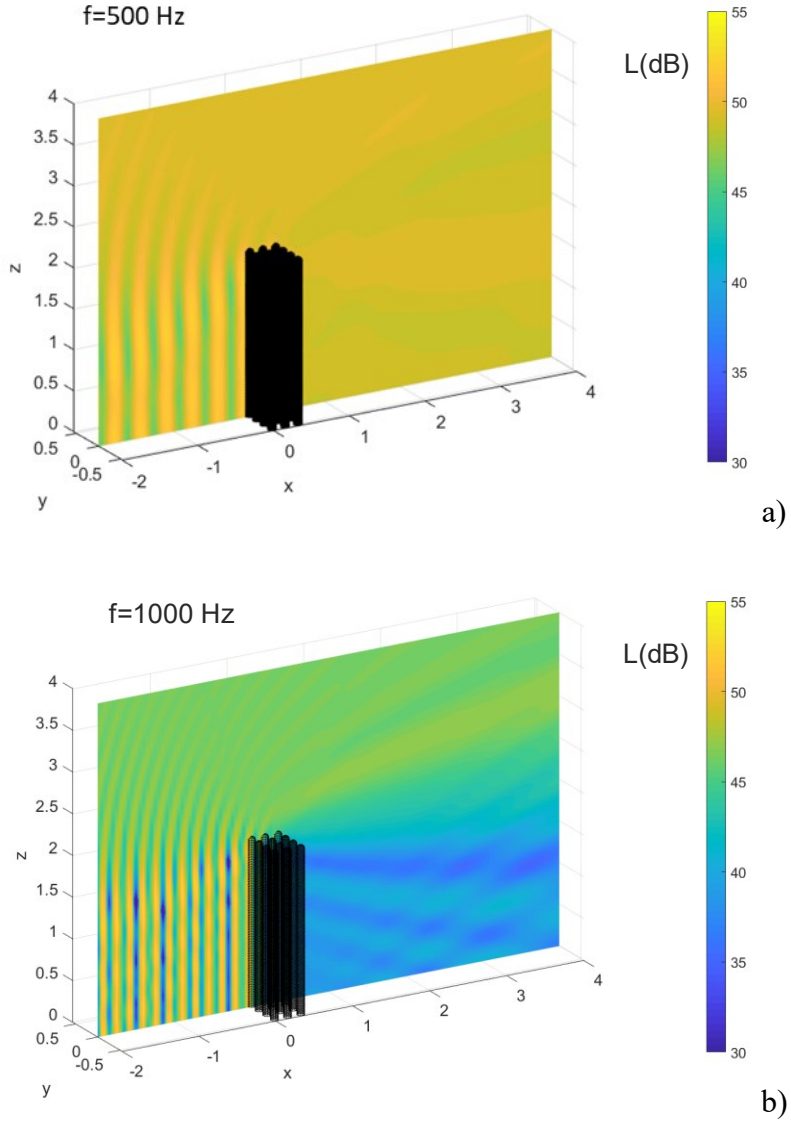

Figure 3 – Sound pressure level around the sonic structure generated by an incident planewave with a frequency of 500 Hz (a) and 1000 Hz (b).

Figure 4 exhibits a set of IL curves computed for rigid sonic crystal structures, for frequencies between 100 Hz and 3150 Hz, for scatterers with different diameters (50%, 75% an 90% of the maximum possible diameter). As can be seen in this figure, as the diameter of the scatterers increases, the insertion loss provided by the barrier becomes higher. In addition, around the frequency of 1000 Hz, the bandgap effect typical of sonic crystals (associated with the Bragg effect) becomes more intense, and at that frequency very little energy is able to travel across the barrier. In the same figure a green line represents the IL predicted for a conventional noise barrier (flat rigid wall, 2.0 m tall).

Comparing the two types of noise barrier clearly distinct behaviours can be observed, with the conventional barrier exhibiting a progressive increase in the performance as higher frequencies are considered, while the sonic crystal clearly show increased performance at specific frequency bands, which can surpass the conventional barrier, but which much lower performance at the remaining frequencies.

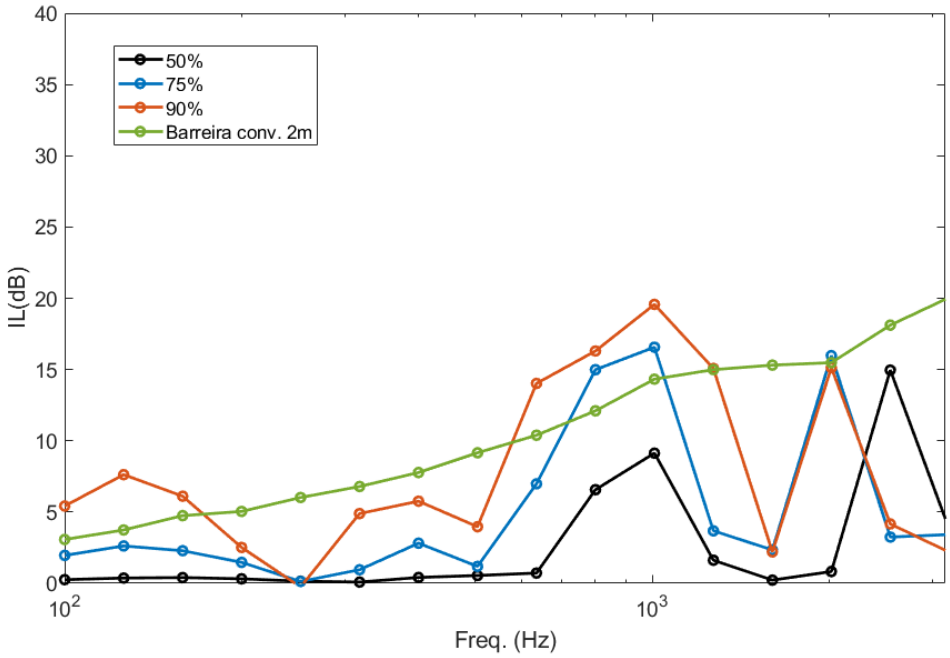

Figure 4 – Insertion loss predicted for the conventional and sonic crystal barriers.

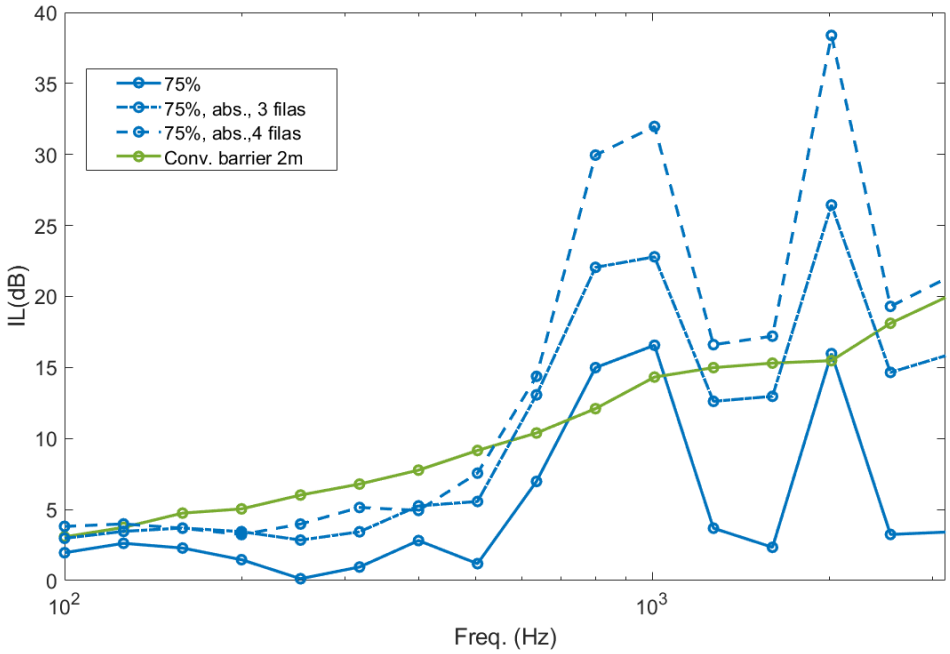

Figure 5 – Insertion loss for sonic crystal barriers with absorbing surface.

In Figure 5 some example results are presented concerning the performance of a sonic crystal barrier with absorbing scatterers. Scatterers with 75% of the maximum possible diameter are considered, and two different sound absorption curves are tested for their surface. The simpler case analysed corresponds to absorption coefficients linearly varying

between 0.1 (at 100 Hz) and 0.5 (at 3150 Hz), for which case barriers with either 3 or 4 lines of scatterers are simulated. Comparing the absorbing barrier with 3 scatterers with and without surface absorption, it becomes clear that a global improvement is visible, throughout the frequency range, and for this case improvements of at least 5 dB are seen above 500 Hz. Even at the Bragg frequency this improvement is quite marked. As an additional row is added, the performance is further improved, and the sonic crystal now performs significantly better than the conventional barrier for all frequencies above 500 Hz. At the Bragg frequency, an insertion loss above 30 dB are registered, which is a very good result for any barrier type. Clearly, the effect of the surface absorption is quite significant, and this type of solution can be of great practical interest.

4. CONCLUSIONS

A numerical implementation of the Method of Fundamental Solutions has been used to study the 3D behaviour of sonic crystal noise barriers. Some results are presented confirming the accuracy of the proposed method. Numerical application results were presented, allowing the identification of the main acoustic features associated with the propagation of sound waves in the presence of such features. Presented simulations also indicate that the effect of the surface absorption is quite significant, and this type of solution can be of great practical interest. Further studies concerning different possibilities to ensure good sound absorption of the scatterers, even at lower frequencies, can be a possible solution to allow even better performance of such structures.

5. ACKNOWLEDGEMENTS

This work was financed by the POCI-01-0247-FEDER-033691 (HLS) Project, cofunded by FEDER funds through COMPETE 2020. This work was also partly financed by FEDER funds through the Competitivity Factors Operational Programme - COMPETE and by national funds through FCT – Foundation for Science and Technology within the scope of the project POCI-01-0145-FEDER-007633 and through the Regional Operational Programme CENTRO2020 within the scope of the project CENTRO-01-0145-FEDER-000006.

The authors also acknowledge COST Action DENORMS CA15125, supported by COST (European Cooperation in Science and Technology).

6. REFERENCES

[1] Kafesaki, M., & Economou, E. N. (1999). Multiple-scattering theory for three-dimensional periodic acoustic composites. Physical review B, 60(17), 11993.

[2] Cao, Y., Hou, Z., & Liu, Y. (2004). Convergence problem of plane-wave expansion method for phononic crystals. Physics Letters A, 327(2-3), 247-253.

[3] Yan, Z. Z., & Wang, Y. S. (2006). Wavelet-based method for calculating elastic band-gaps of two-dimensional phononic crystals. Physical review B, 74(22), 224303.

[4] Cao, Y., Hou, Z., & Liu, Y. (2004). Finite difference time domain method for band-structure calculations of two-dimensional phononic crystals. Solid state communications, 132(8), 539-543.

[5] Li, F. L., Wang, Y. S., Zhang, C., & Yu, G. L. (2013). Band-gap calculations of two-dimensional solid–fluid phononic crystals with the boundary element method. Wave Motion, 50(3), 525-541.

[6] Koussa, F., Defrance, J., Jean, P., & Blanc-Benon, P. (2013). Acoustical efficiency of a sonic crystal assisted noise barrier. Acta acustica united with acustica, 99(3), 399-409.

[7] Karimi, M., Croaker, P., & Kessissoglou, N. (2016). Boundary element solution for periodic acoustic problems. Journal of Sound and Vibration, 360, 129-139.
[8] Castiñeira-Ibáñez, S., Rubio, C., & Sánchez-Pérez, J. V. (2013). Acoustic wave diffraction at the upper edge of a two-dimensional periodic array of finite rigid cylinders. A comprehensive design model of periodicity-based devices. EPL (Europhysics Letters), 101(6), 64002.
[9] Zheng, H., Zhang, C., Wang, Y., Sladek, J., & Sladek, V. (2016). Band structure computation of in-plane elastic waves in 2D phononic crystals by a meshfree local RBF collocation method. Engineering Analysis with Boundary Elements, 66, 77-90.
[10] Yan, Z. Z., Wei, C. Q., Zheng, H., & Zhang, C. (2016). Phononic band structures and stability analysis using radial basis function method with consideration of different interface models. Physica B: Condensed Matter, 489, 1-11.
[11] Golberg, M. A., & Chen, C. S. (1998). The method of fundamental solutions for potential, Helmholtz and diffusion problems. Boundary integral methods-numerical and mathematical aspects, 103-176.
[12] Godinho, L. M. C., Costa, E. G. A., Pereira, A. S. C., & Santiago, J. A. F. (2012). Some observations on the behavior of the method of fundamental solutions in 3D acoustic problems. International Journal of Computational Methods, 9(04), 1250049.
[13] Godinho, L., Redondo, J., & Amado-Mendes, P. (2019). The method of fundamental solutions for the analysis of infinite 3D sonic crystals. Engineering Analysis with Boundary Elements, 98, 172-183.
[14] Redondo, J., Picó, R., Roig, B., & Avis, M. R. (2007). Time domain simulation of sound diffusers using finite-difference schemes. Acta acustica united with acustica, 93(4), 611-622.